

See discussions, stats, and author profiles for this publication at: <https://www.researchgate.net/publication/5511673>

# Orientation of Fluorinated Cholesterol in Lipid Bilayers Analyzed by $^{19}\text{F}$ Tensor Calculation and Solid-State NMR

ARTICLE in JOURNAL OF THE AMERICAN CHEMICAL SOCIETY · MAY 2008

Impact Factor: 12.11 · DOI: 10.1021/ja077580l · Source: PubMed

CITATIONS

11

READS

25

## 5 AUTHORS, INCLUDING:



**Yusuke Kasai**

Tokushima Bunri University

33 PUBLICATIONS 449 CITATIONS

SEE PROFILE



**Tohru Oishi**

Kyushu University

131 PUBLICATIONS 2,354 CITATIONS

SEE PROFILE



**Michio Murata**

Osaka University

224 PUBLICATIONS 7,407 CITATIONS

SEE PROFILE



**Kaoru Nomura**

Suntory Foundation For Life Sciences

14 PUBLICATIONS 352 CITATIONS

SEE PROFILE

## Orientation of Fluorinated Cholesterol in Lipid Bilayers Analyzed by $^{19}\text{F}$ Tensor Calculation and Solid-State NMR

Nobuaki Matsumori,<sup>\*,†</sup> Yusuke Kasai,<sup>†</sup> Tohru Oishi,<sup>†</sup> Michio Murata,<sup>†</sup> and Kaoru Nomura<sup>‡</sup>

*Department of Chemistry, Graduate School of Science, Osaka University, 1-1 Machikaneyama, Toyonaka, Osaka 560-0043, Japan, and Suntory Institute for Bioorganic Research, 1-1-1 Wakayamadai, Shimamoto-Cho, Mishima-Gun, Osaka 618-8503, Japan*

Received October 9, 2007; E-mail: matumori@ch.wani.osaka-u.ac.jp

**Abstract:** 6-F-cholesterol was reported to exhibit biological and interfacial properties similar to unmodified cholesterol. We have also found that 6-F-cholesterol mimicked the cholesterol activity observed in the systems of amphotericin B and lipid rafts. However, to use 6-F-cholesterol as a molecular probe to explore molecular recognition in membranes, it is indispensable to have detailed knowledge of the dynamic and orientation properties of the molecule in membrane environments. In this paper, we present the molecular orientation of 6-F-cholesterol (30 mol %) in dimyristoylphosphatidylcholine (DMPC) bilayers revealed by combined use of  $^{19}\text{F}$  chemical shift anisotropy (CSA),  $^2\text{H}$  NMR, and C–F rotational echo double resonance (REDOR) experiments. The axis of rotation of 6-F-cholesterol was shown to be in a similar direction to that of cholesterol in DMPC bilayers, which is almost parallel to the long axis of the molecular frame. The molecular order parameter of 6-F-cholesterol was determined to be ca. 0.85, which is within the range of reported values of cholesterol. These findings suggest that the dynamic properties of 6-F-cholesterol in DMPC are quite similar to those of unmodified cholesterol; therefore, the introduction of a fluorine atom at C6 has virtually no effect on cholesterol dynamics in membranes. In addition, this study demonstrates the practical utility of theoretical calculations for determining the  $^{19}\text{F}$  CSA principal axes, which would be extremely difficult to obtain experimentally. The combined use of quantum calculations and solid-state  $^{19}\text{F}$  NMR will make it possible to apply the orientation information of  $^{19}\text{F}$  CSA tensors to membrane systems.

### Introduction

Use of  $^{19}\text{F}$  NMR has been of interest for many years in investigating biological systems, due in large part to the experimentally attractive properties of  $^{19}\text{F}$ , including 100% natural abundance, spin  $I = 1/2$ , large magnetogyric ratio, and low background signals in biological samples. In particular, solid-state  $^{19}\text{F}$  NMR has become an indispensable tool for characterizing the orientation and dynamics of membrane-associated peptides.<sup>1</sup> Subsequently, the need for fluorinated compounds suitable for  $^{19}\text{F}$  NMR measurements has also increased. In the course of our studies on amphotericin B, which is a channel-forming antibiotic, and lipid rafts, we used fluorinated derivatives to investigate molecular recognition in bilayer membranes<sup>2–4</sup> and found 6-F-cholesterol **1** to be a successful molecular mimic of cholesterol for investigating intermolecular interactions involving cholesterol. 6-F-cholesterol was originally reported as a growth factor of yeast that has the

activity comparable with cholesterol.<sup>5</sup> Then, Kauffmann et al. studied the air–water interfacial properties of cholesterol and its derivatives<sup>6</sup> and showed the similarity of 6-F-cholesterol to unmodified cholesterol. In our recent experiments, 6-F-cholesterol was shown to reproduce cholesterol activity in the systems of amphotericin B<sup>4</sup> and lipid rafts (to be published in due course). However, to use 6-F-cholesterol as a molecular probe in examining intermolecular recognition in membranes, it is indispensable to have detailed knowledge of its dynamic and orientation properties in membrane environments.

Due to its large anisotropic effect,<sup>1</sup>  $^{19}\text{F}$  chemical shift anisotropy (CSA) seems to be the best choice for obtaining the orientational information of 6-F-cholesterol in membranes. The CSA tensor is defined by three principal values ( $\delta_{11}$ ,  $\delta_{22}$ , and  $\delta_{33}$ ) and three corresponding orthogonal axes, called principal axes.<sup>7</sup> Thus, motion and orientation information with respect to the CSA tensor axes can be obtained by chemical shift measurements. In particular,  $^{13}\text{C}$  and  $^{15}\text{N}$  CSA tensors in peptide bonds are frequently used to assign the alignments of helical

<sup>†</sup> Osaka University.

<sup>‡</sup> Suntory Institute for Bioorganic Research.

- (1) Ulrich, A. S. *Prog. Nucl. Magn. Reson. Spectrosc.* **2005**, *46*, 1–21.
- (2) Matsumori, N.; Umegawa, Y.; Oishi, T.; Murata, M. *Bioorg. Med. Chem. Lett.* **2005**, *15*, 3565–3567.
- (3) Tsuchikawa, H.; Matsushita, N.; Matsumori, N.; Murata, M.; Oishi, T. *Tetrahedron Lett.* **2006**, *47*, 6187–6191.
- (4) Kasai, Y.; Matsumori, N.; Umegawa, Y.; Matsuoka, S.; Ueno, H.; Ikeuchi, H.; Oishi, T.; Murata, M. *Chemistry* **2008**, *14*, 1178–1185.

- (5) Harte, R. A.; Yeaman, S. J.; McElhinney, J.; Suckling, C. J.; Jackson, B.; Suckling, K. E. *Chem. Phys. Lipids* **1996**, *83*, 45–59.
- (6) Kauffman, J. M.; Westerman, P. W.; Carey, M. C. *J. Lipid Res.* **2000**, *41*, 991–1003.
- (7) Duer, M. J. *Introduction to Solid-State NMR Spectroscopy*; Blackwell Publishing: Oxford, UK, 2004.

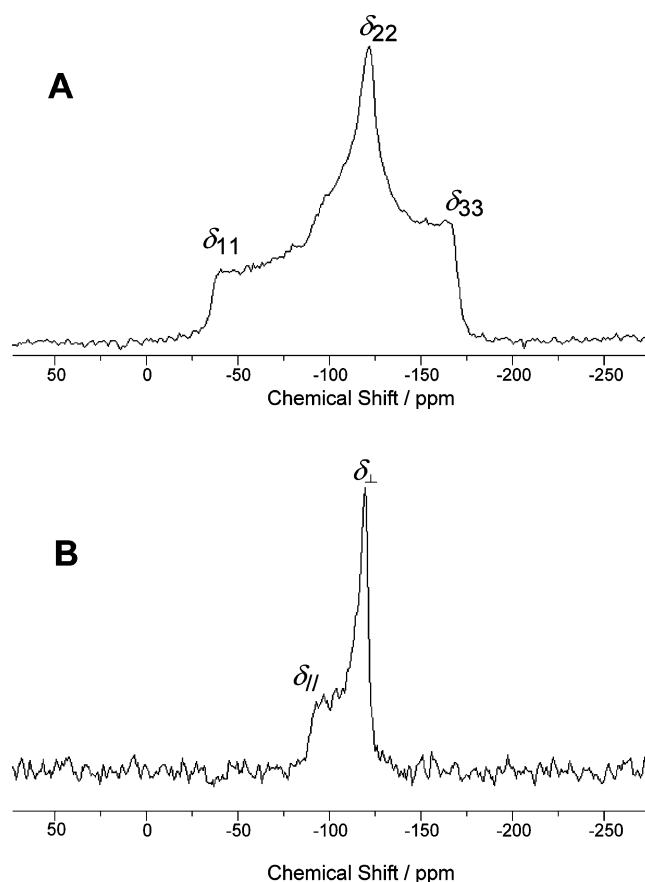
membrane peptides in lipid bilayers.<sup>8–11</sup> However, unlike <sup>13</sup>C and <sup>15</sup>N CSA in peptide bonds that are extensively studied, the <sup>19</sup>F CSA tensor of each compound must be determined prior to utilizing it. While the principal values of the CSA tensor can be conveniently measured with solid-state NMR techniques, the determination of the CSA principal axis orientation in a molecular segment requires more involved methods, such as NMR analysis of a single crystal and comparison with its corresponding X-ray structure. Therefore, CSA tensors of nuclei other than <sup>13</sup>C and <sup>15</sup>N in peptide bonds are seldom used for NMR analyses in biological systems.

Alternatively, a number of papers have recently appeared concerning the calculation of CSA tensors by quantum chemistry methods. For calculation of <sup>19</sup>F CSA tensors,<sup>12,13</sup> Oldfield et al. reported that the gauge including atomic orbitals (GIAO) method combined with Hartree–Fock (HF) calculations correlated well with experimental values in a series of fluorobenzenes.<sup>13</sup> Hence, in this study, we have adopted theoretical calculation as a practical method of determining the <sup>19</sup>F CSA tensor orientation of 6-F-cholesterol. Simultaneously, we have measured static solid-state <sup>19</sup>F NMR of 6-F-cholesterol in dimyristoylphosphatidylcholine (DMPC) bilayers and analyzed the molecular rotation axis in the membrane according to the calculated <sup>19</sup>F CSA tensor. Besides, because the orientation information derived solely from <sup>19</sup>F CSA was not enough to unambiguously specify the rotational axis and the molecular order parameter of 6-F-cholesterol in the membrane, we also measured the intramolecular C–F dipole coupling between 6-F and C5 and the <sup>2</sup>H NMR of [3-<sup>2</sup>H,6-F]cholesterol. On the basis of these data, we report the detailed dynamics and orientation properties of 6-F-cholesterol in DMPC bilayers.

## Results and Discussion

**Preparation of 6-F-cholesterol (1) and [3-<sup>2</sup>H,6-F]Cholesterol (2).** 6-F-cholesterol **1** was prepared using the procedure reported by Harte et al.<sup>5</sup> (Scheme 1). In brief, acetylated cholesterol **4** was subjected to hydroboration and H<sub>2</sub>O<sub>2</sub> oxidation to give alcohol **5**, which was further oxidized to ketone **6**. Fluorination of **6** with diethylaminoethyl sulfur trifluoride (DAST) and subsequent removal of the acetyl group produced 6-F-cholesterol **1** with a moderate yield. [3-<sup>2</sup>H,6-F]Cholesterol **2** was prepared from 6-F-cholesterol **1** by oxidation of 3-OH, and subsequent reduction with NaBD<sub>4</sub>.

**<sup>19</sup>F CSA of 6-F-cholesterol.** We first measured the static solid-state <sup>19</sup>F NMR of 6-F-cholesterol in powder form to obtain <sup>19</sup>F CSA tensor values (Figure 1A). The spectrum was recorded without spinning under <sup>1</sup>H decoupling. To reduce background <sup>19</sup>F signals originating from the Teflon capacitor and other <sup>19</sup>F materials in the NMR probe, we applied the DEPTH method.<sup>14</sup> The obtained spectrum showed a typical powder pattern, from which we extracted the <sup>19</sup>F CSA principal values, as listed in Table 1.

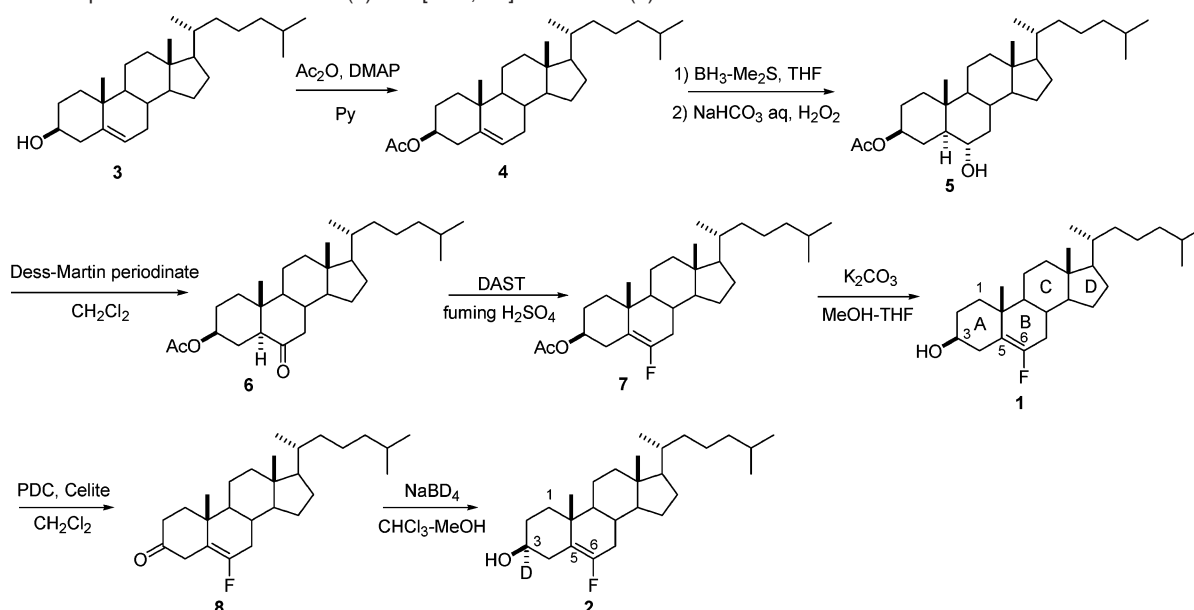


**Figure 1.** Static solid-state <sup>19</sup>F NMR of 6-F-cholesterol in the powder state (A) and in DMPC bilayers at 30 mol % (B). Spectra recorded at 30 °C using the DEPTH method to reduce the background <sup>19</sup>F signals of the NMR probe.<sup>14</sup>

Next, to obtain the <sup>19</sup>F CSA principal axis system with respect to the molecular frame, we calculated the <sup>19</sup>F CSA tensor using the GIAO method.<sup>15</sup> Upon calculation, we used the truncated structure shown in Figure 2 as the input, because 3-OH and the CD rings are considered to have minimal or virtually no effect on 6-F atom, in terms of its electronic state and conformation. Prior to the CSA tensor calculation, we optimized the structure with Becke's three-parameter hybrid functional<sup>16</sup> and the Lee, Yang, and Parr correlation functional (B3LYP)<sup>17</sup> method, using the 6-311G(d) basis set. For <sup>19</sup>F CSA tensor calculations using the GIAO method, Oldfield et al. compared the HF methods with Møller–Plesset (MP) and density-functional theory (DFT) calculations and reported that the results of HF methods correlated best with experimental NMR data.<sup>13</sup> This implies that introduction of the electron correlation does not always enhance the accuracy in <sup>19</sup>F CSA tensor calculations. Hence, we adopted the HF method with a 6-311G++(2d,2p) basis for the GIAO calculation of <sup>19</sup>F CSA. Surprisingly enough, calculated principal values of <sup>19</sup>F CSA were found to be in excellent agreement with the observed ones—within 1 ppm (Table 1). This demonstrated the validity of the input structure and the calculation method. Figure 2 shows the calculated <sup>19</sup>F CSA principal axis directions. The consistency between the experimental and calculated principal values (Table 1) suggests that the theoretical principal axis directions are also highly reliable. In the calculated

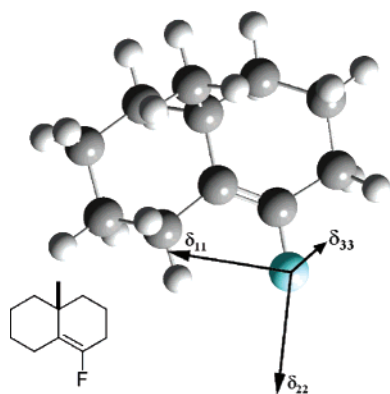
- (8) Davis, J. H.; Auger, M. *Prog. Nucl. Magn. Reson. Spectrosc.* **1999**, *35*, 1–84.
- (9) Bechinger, B.; Sizun, C. *Concepts Magn. Reson. A* **2003**, *18A*, 130–145.
- (10) Yamaguchi, S.; Hong, T.; Waring, A.; Lehrer, R. I.; Hong, M. *Biochemistry* **2002**, *41*, 9852–9862.
- (11) Toraya, S.; Nishimura, K.; Naito, A. *Biophys. J.* **2004**, *87*, 3323–3335.
- (12) Wiberg, K. B.; Kurt W. Zilm, K. W. *J. Org. Chem.* **2001**, *66*, 2809–2817.
- (13) Chan, J. C. C.; Echert, H. *THEOCHEM* **2001**, *535*, 1–8.
- (14) Sanders, L. K.; Oldfield, E. *J. Phys. Chem. A* **2001**, *105*, 8098–8104.
- (15) Cory, D. G.; Ritchey, W. M. *J. Magn. Reson.* **1988**, *80*, 128–132.

- (15) Ditchfield, R. *Mol. Phys.* **1974**, *27*, 789–807.
- (16) Becke, A. D. *J. Chem. Phys.* **1993**, *98*, 5648–5652.
- (17) Lee, C.; Yang, W.; Parr, R. G. *Phys. Rev. B* **1988**, *37*, 785–789.

**Scheme 1.** Preparation of 6-F-cholesterol (**1**) and [3-<sup>2</sup>H,6-F]cholesterol (**2**)**Table 1.** Experimental and Theoretical <sup>19</sup>F CSA Principal Values (ppm) of 6-F-cholesterol

	$\delta_{11}$	$\delta_{22}$	$\delta_{33}$	$\delta_{iso}$
experimental	-40	-123	-167	-110
theoretical <sup>a</sup>	-39.8	-123.9	-166.3	-110

<sup>a</sup> Data were generated using the value for experimental isotropic chemical shift (-110 ppm). Absolute shielding tensors are presented in the Supporting Information.

**Figure 2.** Input structure for CSA tensor calculation and calculated <sup>19</sup>F CSA principal axis directions. The structure was optimized with B3LYP 6-311G(d), and the CSA tensor was calculated with the HF-GIAO method, using the 6-311G++(2d,2p) basis set. The optimized structure is shown.

principal axis system, the  $\delta_{11}$  axis is almost parallel to the C5–C6 bond direction and the  $\delta_{22}$  axis has a direction similar to the C6–F bond.

**<sup>19</sup>F NMR of 6-F-cholesterol in DMPC Bilayers.** With the <sup>19</sup>F CSA principal values and axes available, we measured the static <sup>19</sup>F NMR of 30 mol % 6-F-cholesterol in DMPC bilayers (Figure 1B). The spectrum shows a typical axially symmetric pattern with the two tensor values of -120 and -90 ppm, corresponding to  $\delta_{\perp}$  and  $\delta_{\parallel}$ , respectively. This means that the molecule undergoes a fast axial rotation in the membrane, as in the case of cholesterol. The  $\delta_{\parallel}$  and  $\delta_{\perp}$  values are given as functions of the polar coordinates  $\alpha$  (azimuthal angle) and  $\beta$

(polar angle) connecting the rotation axis and the <sup>19</sup>F CSA tensor axes (Figure 3):<sup>9</sup>

$$\delta_{\parallel} = \delta_{11} \cos^2 \beta + \delta_{22} \sin^2 \alpha \sin^2 \beta + \delta_{33} \sin^2 \beta \cos^2 \alpha \quad (1)$$

and

$$\delta_{\perp} = [\delta_{11} \sin^2 \beta + \delta_{22}(1 - \sin^2 \alpha \sin^2 \beta) + \delta_{33}(1 - \sin^2 \beta \cos^2 \alpha)]/2 \quad (2)$$

Therefore, the anisotropic parameter,  $\Delta\delta = \delta_{\parallel} - \delta_{\perp}$ , is given by

$$\Delta\delta = \delta_{\parallel} - \delta_{\perp} = [\delta_{11}(3 \cos^2 \beta - 1) + \delta_{22}(3 \sin^2 \alpha \sin^2 \beta - 1) + \delta_{33}(3 \sin^2 \beta \cos^2 \alpha - 1)]/2 \quad (3)$$

When introducing the molecular order parameter ( $S_{mol}$ ) to account for the wobbling of the rotation axis with respect to the bilayer normal,<sup>1,18</sup> the observed value of  $\Delta\delta$  is given by

$$\Delta\delta_{obs} = S_{mol} \times \Delta\delta \quad (4)$$

The  $S_{mol}$  parameter varies between 1, wherein there are no molecular oscillations with respect to the rotation axis, and 0, wherein all orientations are allowed, as in a liquid phase. In the following analysis, we assume that the local order parameter,  $S_{loc}$ , is 1, i.e., the internal mobility within the four rings of the sterol is negligible. In effect, Marsan et al. reported that the internal mobility does not need to be included in the calculation of cholesterol.<sup>19</sup> Considering the similarity in the molecular structure of cholesterol and 6-F-cholesterol, it is reasonable to assume the internal mobility is also negligible in 6-F-cholesterol.

Figure 3 shows a contour plot of  $\Delta\delta$  values when varying  $\alpha$  and  $\beta$  angles at a  $S_{mol}$  of 1. For calculation of the contour plot, the experimental values listed in Table 1 were used for  $\delta_{11}$ ,  $\delta_{22}$ , and  $\delta_{33}$  in eq 3. The red lines represent the combinations

(18) Aussenac, F.; Tavares, M.; Dufourc, E. J. *Biochemistry* **2003**, *42*, 1383–1390.

(19) Marsan, M. P.; Muller, I.; Ramos, C.; Rodriguez, F.; Dufourc, E. J.; Czaplicki, J.; Milon, A. *Biophys. J.* **1999**, *76*, 351–359.

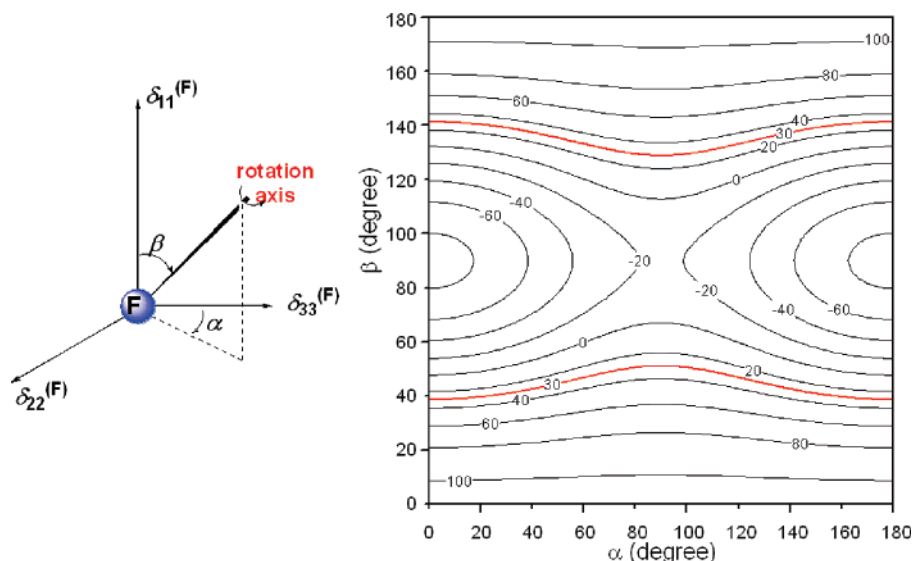


**Figure 3.** Simulated  $\Delta\delta$  values (ppm) of  $^{19}\text{F}$  in 6-F-cholesterol as function of azimuthal angle,  $\alpha$ , and polar angle,  $\beta$ , that relate  $^{19}\text{F}$  CSA tensor orientation with molecular rotation axis. Contour plot drawn for  $S_{\text{mol}} = 1$ . Red lines represent an experimental value of 30 ppm.

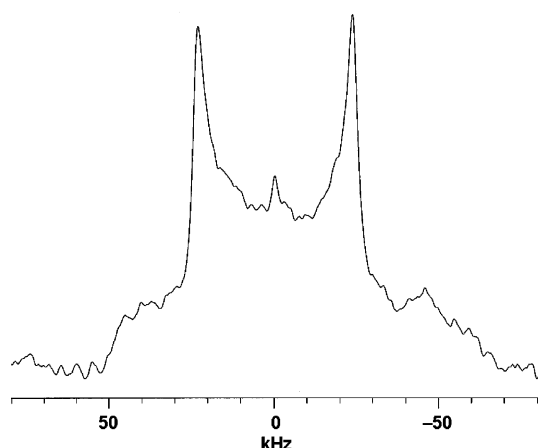


**Figure 4.**  $^2\text{H}$  NMR spectrum of 30 mol %  $[3\text{-}^2\text{H},6\text{-F}]$ cholesterol (**2**) in DMPC. Spectrum recorded at 30 °C, using quadrupolar echo sequence. The quadrupolar splitting  $\Delta\nu$  is 47 kHz.

of  $\alpha$  and  $\beta$  angles that reproduce the experimental  $\Delta\delta$  value of +30 ppm. From the figure, it is clear that while  $\alpha$  can take all values,  $\beta$  is confined between 39° and 51° or between 129° and 141°.

**$^2\text{H}$  NMR of  $[3\text{-}^2\text{H},6\text{-F}]$ Cholesterol in DMPC Bilayers.** To gain further information on the rotation axis of 6-F-cholesterol, we measured solid-state  $^2\text{H}$  NMR using the  $[3\text{-}^2\text{H},6\text{-F}]$ cholesterol **2** prepared above. Quadrupolar splittings, obtained from  $^2\text{H}$  NMR spectra, allow for the determination of the tilt angle of C— $^2\text{H}$  bond with respect to the rotation axis. Figure 4 shows the  $^2\text{H}$  NMR spectrum of **2** in DMPC bilayers. The observed quadrupolar splitting,  $\Delta\nu$ , was 47 kHz, which is significantly reduced from the rigid-limit quadrupolar splitting. This also suggests the rotational averaging in the membrane.

When the motion of the C3— $^2\text{H}$  segment is axially symmetric, the quadrupolar splitting  $\Delta\nu$  of  $^2\text{H}$  NMR is given by<sup>18,20</sup>

$$\Delta\nu = (3/4)A_Q S_{\text{mol}}(3 \cos^2 \theta - 1)/2 \quad (5)$$

where  $(3/4)A_Q$  is the rigid-limit quadrupolar splitting, and we used 114 kHz for  $(3/4)A_Q$  based on our experimental data of

solid powder  $[3\text{-}^2\text{H}]$ cholesterol (Figure S3 in the Supporting Information).  $S_{\text{mol}}$  is the molecular order parameter, as described above, and  $\theta$  is the angle formed by the C3— $^2\text{H}$  bond and the axis of motion. Given the angles ( $l, m, n$ ) of the C3— $^2\text{H}$  bond with respect to the  $^{19}\text{F}$  principal axis system ( $\delta_{11}, \delta_{22}, \delta_{33}$ ) of 6-F-cholesterol (Figure 5),  $\theta$  is defined by<sup>21</sup>

$$\cos \theta = \cos l \cos \beta + \cos m \sin \alpha \sin \beta + \cos n \cos \alpha \sin \beta \quad (6)$$

where  $\alpha$  and  $\beta$  are the polar coordinates of the rotation axis in the  $^{19}\text{F}$  principal axis frame (Figure 5). In this approach, we added 3-OH to the structure of Figure 2 and extracted ( $l, m, n$ ) angles as 116.8°, 88.3°, and 153.1°, respectively. Using eqs 5 and 6, quadrupolar splittings  $\Delta\nu$  can be related to  $\alpha$  and  $\beta$ . Figure 5 shows the calculated quadrupolar splittings  $\Delta\nu$  as a function of  $\alpha$  and  $\beta$  at a  $S_{\text{mol}}$  of 1. The red and blue lines reproduce the experimental value of 47 kHz. Note that although the sign of the experimental quadrupolar splitting is unknown, the term  $(3 \cos^2 \theta - 1)$  in eq 5 is negative when  $\theta$  is larger than the magic angle (54.7°) and vice versa. Assuming that the rotation axis is nearly along the molecular long axis, as in the case of cholesterol, the angle  $\theta$  between the C3— $^2\text{H}$  bond and the rotation axis should be larger than the magic angle, and therefore,  $\Delta\nu$  should be negative. Thus, we deduced that the red contour lines representing  $\Delta\nu$  of −47 kHz are more reasonable.

**C—F Dipole Coupling of 6-F-cholesterol in DMPC Bilayers.** To further specify the rotational axis direction and the molecular order parameter  $S_{\text{mol}}$  of 6-F-cholesterol in DMPC bilayers, we measured intramolecular C—F dipole coupling, using the C—F rotational echo double resonance (REDOR) method.<sup>22</sup> For this purpose, we chose the dipole interaction between C5 and 6-F, because carbon signals other than for C5 and C6 are overlapped in the REDOR spectra and because the dipole coupling of directly bonded C6—F is too large to detect with the REDOR method.

(20) Shaikh, S. R.; Cherezov, V.; Caffrey, M.; Soni, S. P.; LoCasio, D.; Stillwell, W.; Wassall, S. R. *J. Am. Chem. Soc.* **2006**, *128*, 5375–5383.

(21) Dufourc, E. J.; Parish, E. J.; Chitrakorn, S.; Smith, C. P. *Biochemistry* **1984**, *23*, 6062–6071.

(22) Gullion, T.; Schaefer, J. J. *Magn. Reson.* **1989**, *81*, 196–200.



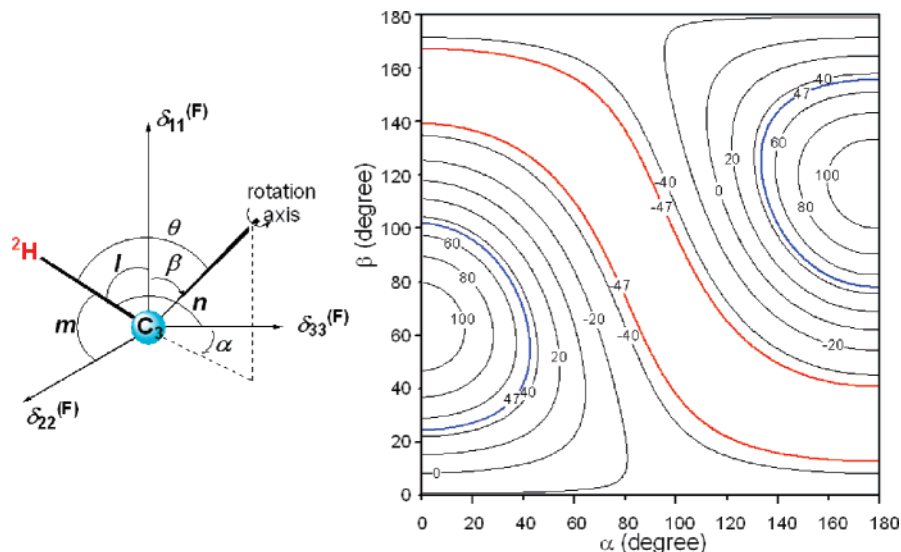


**Figure 5.** Simulated  $\Delta\nu$  values (kHz) of  $^2\text{H}$  NMR in  $[\text{3-}^2\text{H},\text{6-F}]\text{cholesterol}$  (**2**) as a function of azimuthal angle  $\alpha$  and polar angle  $\beta$  that relate  $^{19}\text{F}$  CSA tensor orientation with molecular rotation axis. Angles  $l$ ,  $m$ , and  $n$  are  $116.8^\circ$ ,  $88.3^\circ$ , and  $153.1^\circ$ , respectively. Contour plot drawn for  $S_{\text{mol}} = 1$ . Although the red and blue contour lines agree with the experimental value (47 kHz), red lines are more probable, as deduced from the angle between the  $\text{C3}-^2\text{H}$  bond and the rotation axis (see the text).

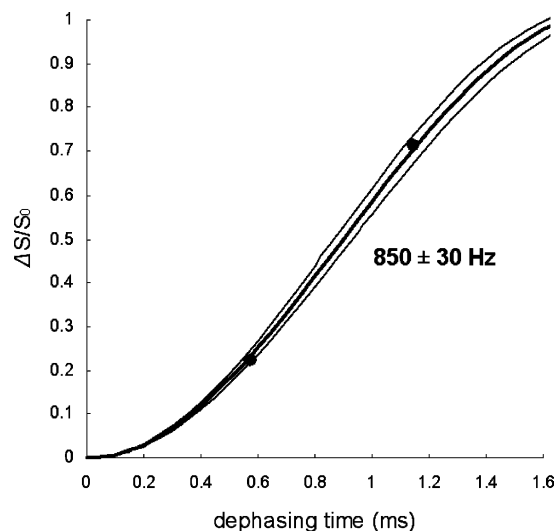


**Figure 6.** Experimental REDOR dephasing values ( $\Delta S/S_0$ ) for C5–F (solid circle) of 30 mol % 6-F-cholesterol in DMPC bilayers. Theoretical dephasing curves of 820 Hz, 850 Hz (bold line), and 880 Hz are depicted to determine the C5–F dipole coupling constant.

Figure 6 plots the experimental REDOR dephasing values ( $\Delta S/S_0$ ) between C5 and 6-F of **1** in DMPC bilayers. As shown in Figure 6, only two dephasing times could be measured, because the buildup of dephasing was steep due to the large C–F dipolar coupling. Nevertheless, the dipole coupling value was estimated to be 850 Hz by comparison with theoretical dephasing curves, as depicted in Figure 6.

Dipolar couplings depend on internuclear distance as well as molecular motion. For a fixed internuclear distance, such as C5–F in **1**, reduction in the coupling strength from its rigid-lattice value is caused only by motional averaging. When the C5–F vector is rotating around an axis, the measured dipolar coupling constant is given by the following equation<sup>1</sup>

$$D_{\text{C-F}} = D_{\text{static}} S_{\text{mol}} (3 \cos^2 \phi - 1)/2 \quad (7)$$

where  $\phi$  is the angle between the C5–F vector and rotation axis.  $D_{\text{static}}$  denotes the dipolar coupling constant for static C5–

F, which was calculated to be 2216 Hz based on the C5–F internuclear distance of 2.341 Å, as determined from the optimized structure shown in Figure 2. As in eq 6, angle  $\phi$  is related to  $\alpha$  and  $\beta$  as follows:

$$\cos \phi = \cos p \cos \beta + \cos q \sin \alpha \sin \beta + \cos r \cos \alpha \sin \beta \quad (8)$$

In this equation,  $p$ ,  $q$ , and  $r$  represent the angles of C5–F with respect to the  $^{19}\text{F}$  CSA principal axes ( $\delta_{11}$ ,  $\delta_{22}$ ,  $\delta_{33}$ ) (Figure 7), which were extracted from Figure 2 as  $138.2^\circ$ ,  $48.5^\circ$ , and  $94.4^\circ$ , respectively. Using eqs 7 and 8, we calculated  $D_{\text{C-F}}$  values for various  $\alpha$  and  $\beta$  angles (Figure 7). The red and blue contour lines in Figure 7 reproduce the experimental value of 850 Hz.

**Determination of  $\alpha$  and  $\beta$  Angles and Molecular Order Parameter  $S_{\text{mol}}$ .** On the basis of the above results, we can specify  $\alpha$  and  $\beta$  angles, and the molecular order parameter  $S_{\text{mol}}$  of 6-F-cholesterol in DMPC bilayers. However, as shown in Figure 8a, a simple superposition of the contour lines agreeing with the experimental values does not give a single intersection point. This is because the contour plots were calculated without accounting for the molecular order parameter  $S_{\text{mol}}$  that represents wobbling of the rotation axis with respect to the membrane normal. In other words, the  $S_{\text{mol}}$  is not unity in this system. In fact, reported  $S_{\text{mol}}$  values range from 0.79 to 0.96 for unmodified cholesterol in DMPC bilayers.<sup>19,21,23</sup> Hence, we varied  $S_{\text{mol}}$  values such that the contour lines derived from the three experiments meet at a single point. Note that the molecular order parameter  $S_{\text{mol}}$  in this system must be greater than 0.82, which corresponds to the ratio between the maximum  $^2\text{H}$  NMR quadrupolar coupling of 57 kHz (one-half of the static quadrupolar coupling 114 kHz) and the observed value of 47 kHz. If  $S_{\text{mol}}$  was less than 0.82, quadrupolar couplings before being scaled by  $S_{\text{mol}}$  would exceed the maximum value of 57 kHz. By changing  $S_{\text{mol}}$  values from 0.82 to 1.0, two solutions of  $\alpha$ ,  $\beta$ , and  $S_{\text{mol}}$  could be found:  $\alpha = 128^\circ$ ,  $\beta = 42^\circ$ ,  $S_{\text{mol}} = 0.83$  (Figure 8b) and  $\alpha = 32^\circ$ ,  $\beta = 140^\circ$ ,  $S_{\text{mol}} = 0.85$  (Figure 8c).

(23) Weisz, K.; Grobner, G.; Mayer, C.; Stohrer, J.; Kothe, G. *Biochemistry* **1992**, *31*, 1100–1112.

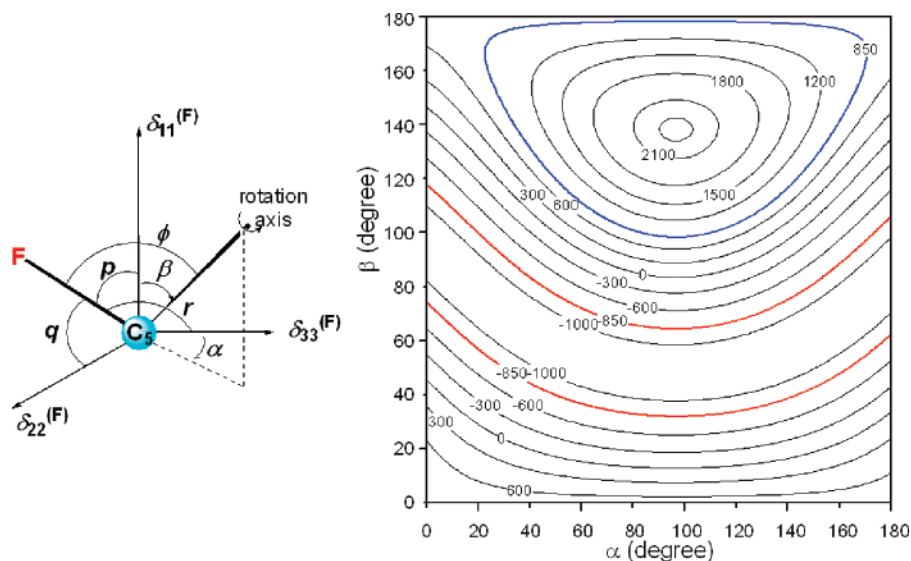


**Figure 7.** Simulated C–F dipole coupling values (Hz) between C5 and F of 6-F-cholesterol as a function of azimuthal angle  $\alpha$  and polar angle  $\beta$  that relate  $^{19}\text{F}$  CSA tensor orientation with molecular rotation axis. Angles  $p$ ,  $q$ , and  $r$  are  $138.2^\circ$ ,  $48.5^\circ$ , and  $94.4^\circ$ , respectively. Contour plot drawn for  $S_{\text{mol}} = 1$ . The red and blue contour lines agree with the experimental value (850 Hz).

Figure 9 shows the orientations of the rotational axes obtained from Figure 8. It can be postulated that the rotational axis of 6-F-cholesterol should be approximately along the long axis of the molecular frame. As seen in Figure 9, the rotation axis derived from Figure 8c is not directed along the molecular long axis, while that derived from Figure 8b appears to be almost parallel to the long axis. Therefore, we concluded that the axis from Figure 8b ( $\alpha = 128^\circ$ ,  $\beta = 42^\circ$ ,  $S_{\text{mol}} = 0.83$ ) is the rotational axis of 6-F-cholesterol in DMPC bilayers.

Now, we address possible errors in the determination of rotational orientation and the molecular order parameter. The evaluation of the C5–F dipole coupling constant seems to cause experimental error, because, as shown in Figure 6, the value was elucidated from only two points of the REDOR measurements. However, the experimental dephasing values fall completely between the theoretical curves of 820 and 880 Hz; therefore, the maximum possible deviation of the C5–F dipole coupling constant is estimated to be  $\pm 30$  Hz. We also evaluated the uncertainties in the other data as follows:  $\Delta\delta = +30 \pm 2$  ppm and  $\Delta\nu = -47 \pm 1$  kHz. We then repeated the above analysis to include these errors. Figure 10 shows the superposition of three contour maps for  $S_{\text{mol}} = 0.89$  and  $0.81$  ( $S_{\text{mol}}$  values less than 0.81 do not give the blue contours corresponding to quadrupolar coupling). Between these  $S_{\text{mol}}$  values, the three contours can have intersections. For  $S_{\text{mol}} = 0.89$  (Figure 10a), the intersection occurs at  $\alpha = 140^\circ$  and  $\beta = 41^\circ$  and for  $S_{\text{mol}} = 0.81$  at  $\alpha = 116^\circ$  and  $\beta = 45^\circ$  (Figure 10b). As seen from the figure,  $\beta$  is relatively tolerant with respect to experimental errors, while  $\alpha$  is more sensitive. On the basis of this consideration, the  $\alpha$ ,  $\beta$ , and  $S_{\text{mol}}$  values are rewritten with uncertainties as follows:  $\alpha = 128^\circ \pm 12^\circ$ ,  $\beta = 42^\circ \pm 3^\circ$ , and  $S_{\text{mol}} = 0.85 \pm 0.04$ .

Another possible source of error in the analysis might be the inaccuracy of the calculated  $^{19}\text{F}$  CSA tensor orientations. However, judging from the good coincidence between the experimental and calculated principal values, as seen in Table 1, the error in the calculated tensor orientation would be within the error generated during measurement. In relation to the calculation of  $^{19}\text{F}$  CSA tensor, we have to refer to possible

change in the CSA tensor orientation and values when in the membrane environment. It is known that  $^{19}\text{F}$  chemical shifts are influenced by dielectric constants. In fact, the dielectric constant in the polar region of lipids is thought to be around 10,<sup>24</sup> which might induce the  $^{19}\text{F}$  chemical shift change. The quantum calculation of the effect of dielectric constant on the  $^{19}\text{F}$  CSA is beyond the scope of this paper; however, according to Abraham et al.,<sup>25</sup> the shift of  $^{19}\text{F}$  CS induced by the dielectric constant of 10 is at most 2 ppm. As mentioned above, we already took 2 ppm as the experimental uncertainty of  $^{19}\text{F}$  CSA measurements. In addition, the isotropic  $^{19}\text{F}$  chemical shift of 6-F-cholesterol in the DMPC membrane can be calculated to be  $\delta_{\text{iso}} = (2\delta_{\perp} + \delta_{\parallel})/3 = -110$  ppm, where  $\delta_{\perp} = -120$  ppm and  $\delta_{\parallel} = -90$  ppm (Figure 1B). This value completely coincides with that in powder form (Table 1), which also suggests that the change in the principal values and the CSA tensor orientation caused by interactions of the molecule with the membrane is, if present, within the experimental error.

**Comparison with Unmodified Cholesterol in DMPC Bilayers.** There are two reports on the rotational axis of 30 mol % cholesterol in DMPC bilayers at  $30^\circ\text{C}$ .<sup>19,21</sup> Figure 11 shows an overlay of the reported rotation axes of unmodified cholesterol and the result of 6-F-cholesterol obtained in this study. The orientation of 6-F-cholesterol falls between the two reported rotation axes of unmodified cholesterol. The difference between the angle obtained in this study and that by Dufourc et al.<sup>21</sup> is  $5^\circ$ , and that obtained by Marsan et al.<sup>19</sup> is  $20^\circ$ . This suggests that the rotational orientation of 6-F-cholesterol is almost parallel to that of unmodified cholesterol.

Next, we compared the molecular order parameter  $S_{\text{mol}}$  of 6-F-cholesterol with that of unmodified cholesterol in DMPC bilayers. The molecular order parameter  $S_{\text{mol}}$  is an accurate descriptor of the wobbling in a cone of rigid moieties. Dufourc et al. reported  $S_{\text{mol}} = 0.79$  for 30 mol % cholesterol in DMPC at  $30^\circ\text{C}$ ,<sup>21</sup> while Marsan reported 0.96 for the same condition.<sup>19</sup>

(24) Sengupta, D.; Meinhold, L.; Langosch, D.; Ullmann, G. M.; Smith J. C. *Proteins* **2005**, 58, 913–922.

(25) Abraham, R. J.; Wileman, D. F. *J. Chem. Soc., Perkin Trans. 2* **1973**, 1521–1526.

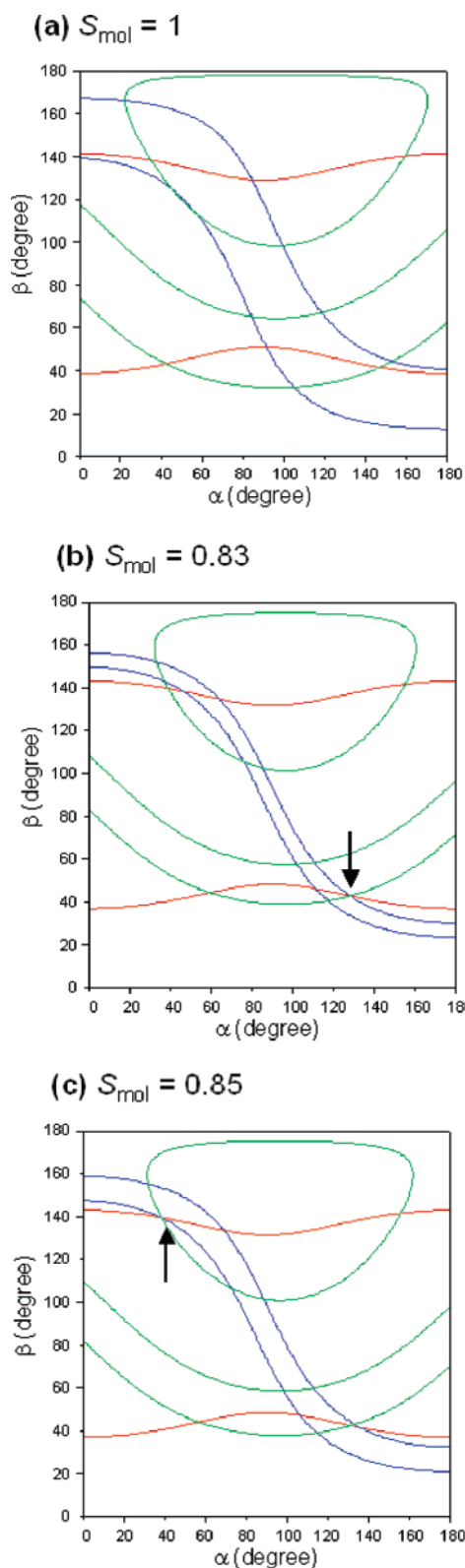


**Figure 8.** Superpositions of contour lines derived from  $^{19}\text{F}$  CSA (red),  $^2\text{H}$  NMR (blue), and C-F dipole coupling (green) for  $S_{\text{mol}} = 1.0$  (a), 0.83 (b), and 0.85 (c). In parts b and c, the three contour lines meet at a single intersection point, giving two solutions of  $\alpha$ ,  $\beta$ , and  $S_{\text{mol}}$ :  $\alpha = 128^\circ$ ,  $\beta = 42^\circ$ ,  $S_{\text{mol}} = 0.83$  (b) and  $\alpha = 32^\circ$ ,  $\beta = 140^\circ$ ,  $S_{\text{mol}} = 0.85$  (c).

Weitz et al. reported 0.85 for 40 mol % cholesterol in DMPC at ambient temperature.<sup>23</sup> In spite of some disagreement in the reported molecular order parameters for cholesterol in DMPC, all these values suggest that the amplitude of cholesterol

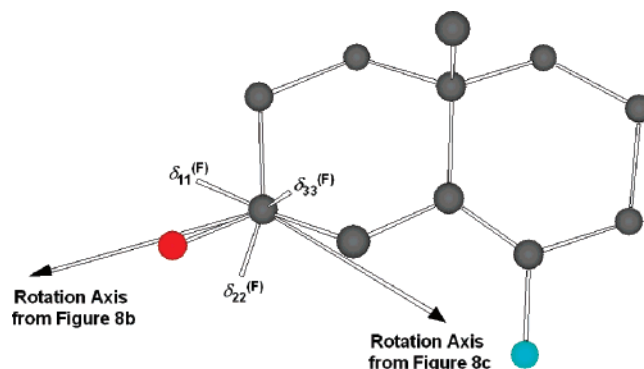


**Figure 9.** Two rotational axes obtained from Figure 8b,c.

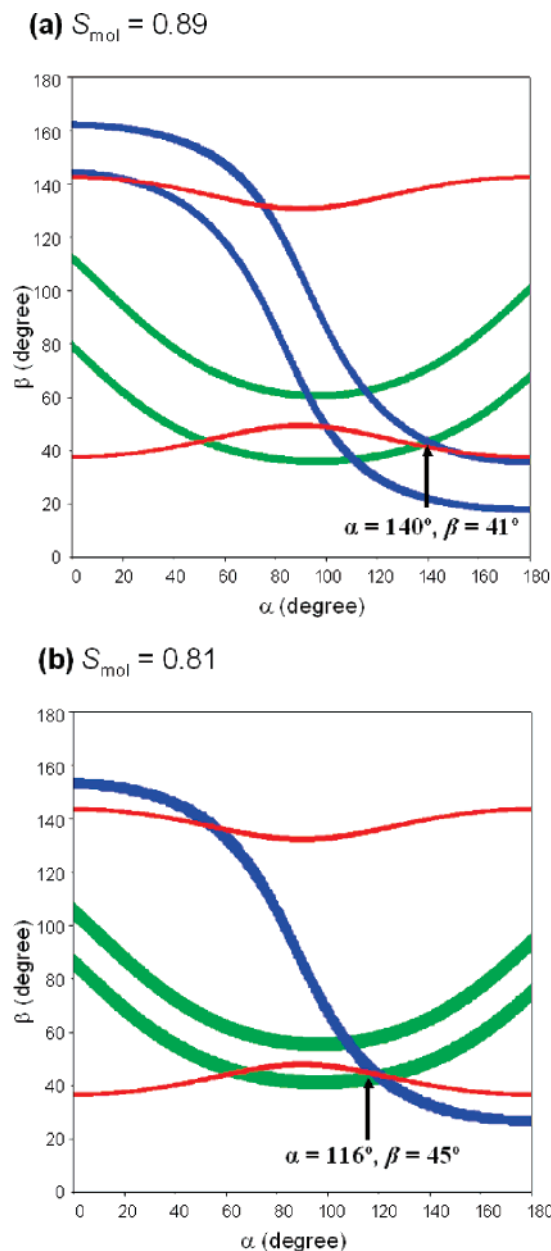


**Figure 10.** Superpositions of contour maps (after including experimental errors) derived from  $^{19}\text{F}$  CSA (red),  $^2\text{H}$  NMR (blue), and C-F dipole coupling (green) for (a)  $S_{\text{mol}} = 0.89$  and (b)  $S_{\text{mol}} = 0.81$ .

wobbling in the membrane is small. With respect to 6-F-cholesterol, the molecular order parameter  $S_{\text{mol}}$  (ca. 0.85) falls within the range of the reported values for unmodified chole-



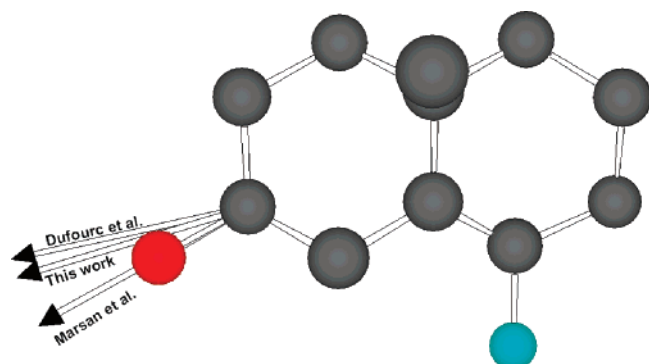


**Figure 11.** Rotational axis orientations for 30 mol % unmodified cholesterol and 6-F-cholesterol in DMPC bilayers at 30 °C. Data for cholesterol were reported by Dufourc et al.<sup>21</sup> and Marsan et al.<sup>19</sup>

terol ( $S_{\text{mol}} = 0.79\text{--}0.96$ ), thus suggesting a small wobbling in DMPC bilayers. In fact, a  $S_{\text{mol}}$  value of 0.85 leads to a cone semiangle of  $13^\circ$  for the oscillations, when assuming a Gaussian distribution of the wobbling angle.<sup>20,26</sup>

Note that the above analysis using the order parameter  $S_{\text{mol}}$  assumes an axial symmetry of the wobbling motion of 6-F-cholesterol in the membrane. If not, a more strict analysis, Saupe order tensor analysis, would be needed.<sup>27</sup> In the case of cholesterol in DMPC bilayers, the wobbling motion is reported to be nearly axial symmetric;<sup>19,27</sup> therefore, the  $S_{\text{mol}}$  analysis can be safely applied.<sup>19</sup> Then, to see the similarity in wobbling motion of cholesterol and 6-F-cholesterol, we have measured the  $^2\text{H}$  NMR of  $[3\text{-}^2\text{H}]\text{cholesterol}$  in DMPC bilayers (Figure S3 in the Supporting Information) and compared the quadrupolar splitting of  $[3\text{-}^2\text{H}]\text{cholesterol}$  (46 kHz) with that of  $[3\text{-}^2\text{H}, 6\text{-F}]\text{cholesterol}$  (47 kHz, Figure 4). The result strongly suggests that the wobbling motion of 6-F-cholesterol is virtually identical to that of cholesterol, thus ensuring the application of the  $S_{\text{mol}}$  analysis to 6-F-cholesterol.

The above findings show that the motional properties of 6-F-cholesterol in DMPC bilayers are quite similar to those of unmodified cholesterol. In other words, the introduction of a fluorine atom at C6 of cholesterol has minimal or virtually no effect on the dynamics of cholesterol in membranes. This is probably due to the small atomic size of the fluorine atom next to the hydrogen atom.

Although at present we have no direct data on the immersion depth of 6-F-cholesterol in the DMPC membrane, previous reports showed that C6 of unmodified cholesterol to be in the polar region of the DMPC bilayers.<sup>28</sup> Considering the well-known nonmiscibility of fluorine in hydrocarbon chains, it seems reasonable to assume that the fluorine of 6-F-cholesterol is also in the polar region. In effect, it was reported that the fluorine atom of 6-F-cholesterol in a membrane was strongly affected by paramagnetic oxygen existing outside the membrane,<sup>29</sup> supporting the vicinity of the fluorine to the membrane surface.

Figure 12 represents the dynamics of 6-F-cholesterol in DMPC bilayers revealed by current data, together with the estimated immersion depth in the membrane. The axis of

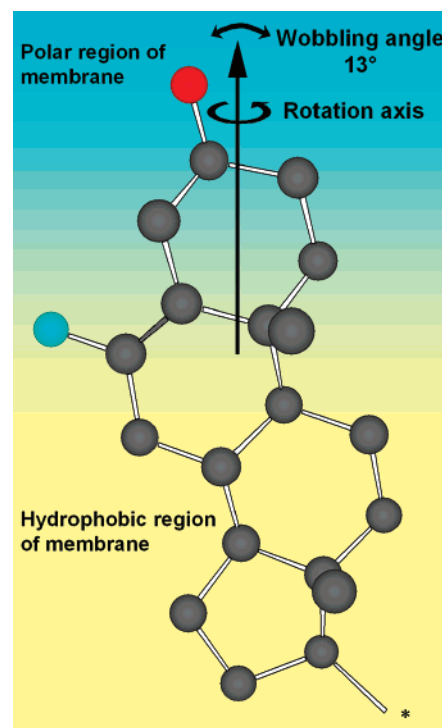


**Figure 12.** Representation of rotational axis orientation and its wobbling for 6-F-cholesterol in DMPC bilayers. \*The side chain is omitted.

motional averaging lies along the long axis of the molecule, and the molecular order parameter of ca. 0.85 indicates a small wobbling of the axis; the cone semiangle of the wobbling is  $13^\circ$ .

Here we will discuss the ordering effect of 6-F-cholesterol on membranes. As described in the introduction, Kauffmann et al. measured the air–water interfacial properties of POPC membranes containing cholesterol or 6-F-cholesterol using a Langmuir–Pockels surface balance and showed that 6-F-cholesterol preserves the interfacial properties of cholesterol, including molecular size, orientation, intercalation into and condensation of POPC membranes.<sup>6</sup> Recently, we have also measured the fluorescent anisotropy of sphingomyelin membranes containing 6-F-cholesterol or unmodified cholesterol and found that both sterols have virtually identical ordering effect on the sphingomyelin membrane (to be published in due course). These data are not for the DMPC membranes, but they strongly support that 6-F-cholesterol has the same ordering effect on membranes as cholesterol.

As mentioned in the Introduction, fluorinated compounds are expected to be versatile tools in investigating biological systems using  $^{19}\text{F}$  NMR. This study shows the potential utility of 6-F-cholesterol as a molecular probe for examining intermolecular recognitions relating to cholesterol. In fact, we have found that sphingomyelin and 6-F-cholesterol, like cholesterol, form a liquid-ordered membrane (manuscript in preparation), which is considered closely related to lipid raft systems in biological membranes.<sup>30</sup> We are currently investigating not only dynamics and orientation of 6-F-cholesterol in sphingomyelin but also intermolecular interactions between 6-F-cholesterol and sphingomyelin.

- (26) Oldfield, E.; Meadows, M.; Rice, D.; Jacobs, R. *Biochemistry* **1978**, *17*, 2727–2740.  
 (27) Sternberg, U.; Witter, R.; Ulrich, A. S. *J. Biomol. NMR* **2007**, *38*, 23–39.  
 (28) Leonard, A.; Escribe, C.; Laguerre, M.; Pebay-Peyroula, E.; Neri, W.; Pott, T.; Katsaras, J.; Dufourc, E. J. *Langmuir* **2001**, *17*, 2019–2030. Villalain J. *Eur. J. Biochem.* **1996**, *241*, 586–593.  
 (29) Prosser, R. S.; Luchette, P. A.; Westerman, P. W.; Rozek, A.; Hancock, R. E. W. *Biophys. J.* **2001**, *80*, 1406–1416.

- (30) Simons, K.; Ikonen, E. *Nature* **1997**, *387*, 569–572.

## Conclusion

In this study, we succeeded in determining the molecular orientation of 6-F-cholesterol in DMPC bilayers by the combined use of  $^{19}\text{F}$  CSA,  $^2\text{H}$  NMR, and C–F REDOR experiments. The rotational angle of 6-F-cholesterol was shown to be close to that of cholesterol in DMPC bilayers. In addition, the molecular order parameter of 6-F-cholesterol is within the range of reported values of cholesterol. These facts suggest that the dynamic properties of 6-F-cholesterol are quite similar to those of unmodified cholesterol. In other words, the introduction of fluorine at C6 has virtually no effect on cholesterol dynamics in membranes, possibly due to the small van der Waals radius of the fluorine atom. Together with our recent finding that 6-F-cholesterol and sphingomyelin form lipid rafts (manuscript in preparation), this study shows the potential utility of 6-F-cholesterol as a versatile tool to probe molecular recognition in lipid rafts and other membrane systems.

In addition to determining 6-F-cholesterol dynamics in a membrane, we devised a method that uses the  $^{19}\text{F}$  CSA tensor to obtain orientation information and demonstrated the validity of the method. In particular, theoretical calculation was shown to be a powerful method of elucidating  $^{19}\text{F}$  CSA tensor directions, which would otherwise be extremely difficult to determine experimentally. The combined use of quantum calculations and solid-state  $^{19}\text{F}$  NMR will make it possible to utilize  $^{19}\text{F}$  CSA tensors of a wide variety of fluorinated compounds for dynamic and orientation studies in membrane environments.

## Experimental Section

**Materials.** Cholesterol, pyridinium dichromate (PDC), and Celite were purchased from Nakarai Tesque (Kyoto, Japan). 1,2-Dimyristoyl-*sn*-glycero-3-phosphocholine (DMPC) was purchased from Avanti Polar Lipid (Alabaster, AL), and  $\text{NaBD}_4$  was from Cambridge Isotope Laboratory (Andover, MA). Deuterium water was purchased from Euriso-Top, and deuterium-depleted water was from Isotec Inc. (Miamisburg, OH). All other chemicals were obtained from standard vendors. Thin-layer chromatography (TLC) was performed on a glass plate precoated with silica gel (Merck Kieselgel 60 F254). Column chromatography was performed with silica gel 60 (Merck, particle size 0.063–0.200 mm, 60–230 mesh). Solution NMR spectra were recorded on a GSX-500 spectrometer (JEOL), and high-resolution MS was measured on a QSTAR Elite (Applied Biosystems).

**Preparation of 3-Keto-6-F-5-cholestene (8).** 6-F-cholesterol (**1**) was prepared from cholesterol by the procedure reported by Harte et al.<sup>5</sup> Pyridinium dichromate (67.0 mg, 178  $\mu\text{mol}$ ) was added to a suspension of 6-F-cholesterol (**1**) (59.3 mg, 147  $\mu\text{mol}$ ) and Celite (100 mg) in dry  $\text{CH}_2\text{Cl}_2$  (10 mL). After being stirred at 25  $^\circ\text{C}$  for 16 h, the mixture was filtered through Celite, and the filtrate was concentrated by evaporation. The residue was purified by  $\text{SiO}_2$  column chromatography (hexane/ethyl acetate = 10/1) to afford ketone **8** as a white powder (13.7 mg, 34.1  $\mu\text{mol}$ , 23%):  $R_f$  = 0.71 (hexane/ethyl acetate = 3/1);  $^1\text{H}$  NMR (500 MHz,  $\text{CDCl}_3$ )  $\delta$  3.45 (1H, d,  $J$  = 18.9 Hz), 2.85 (1H, m), 2.45 (1H, m), 2.31 (1H, m), 2.15 (1H, m), 2.05 (2H, m), 1.85 (2H, m), 1.68 (1H, m), 0.96–1.62 (16H, m), 1.14 (3H, s), 0.91 (3H, d,  $J$  = 6 Hz), 0.85 (6H, d,  $J$  = 6.5 Hz), 0.69 (3H, s).

**Preparation of [3- $^2\text{H}$ ,6-F]Cholesterol 2.** 3-Keto-6-F-5-cholestene (**8**) (13.7 mg, 34.1  $\mu\text{mol}$ ) was dissolved in 1.5 mL of  $\text{MeOH}-\text{CHCl}_3$  (2:1), and to the solution was added  $\text{NaBD}_4$  (5.0 mg, 120  $\mu\text{mol}$ ). After being stirred for 2 h at room temperature, the solvent was removed by evaporation, and the residue was purified by  $\text{SiO}_2$  column chromatography (hexane/ethyl acetate = 10/1) to afford **2** (4.6 mg, 11.4  $\mu\text{mol}$ , 34%) as a white powder:  $R_f$  = 0.45 (hexane/ethyl acetate = 3/1);  $^1\text{H}$

NMR (500 MHz,  $\text{CDCl}_3$ )  $\delta$  3.02 (1H, dd,  $J$  = 13, 2.5 Hz), 2.08 (1H, m), 2.00 (1H, m), 1.70–1.95 (5H, m), 0.95–1.65 (20H, m), 0.98 (3H, s, 3H), 0.89 (3H, d,  $J$  = 6 Hz), 0.84 (6H, d,  $J$  = 6.5 Hz), 0.70 (3H, s); HRMS (ESI-TOF) calcd for  $\text{C}_{27}\text{H}_{44}\text{DOFNa}^+$  [(M+Na) $^+$ ] 428.3408, found 428.3418.

**Computational Method.** All calculations were carried out using Gaussian 03W<sup>31</sup> (Gaussian Inc.) on a Windows XP computer. For the geometry optimization, we utilized Becke's three-parameter hybrid functional<sup>16</sup> and the Lee, Yang, and Parr correlation functional (B3LYP)<sup>17</sup> method with a uniform 6-311G(d) basis set. Subsequent shielding calculation was done with Hartree–Fock gauge including atomic orbitals (HF-GIAO) method using a uniform 6-311++G(2d,2p) basis set. The input structure shown in Figure 2 was generated in GaussView3.0 software (Gaussian Inc.), and the output structure was visualized in GaussView or Chem3D (CambridgeSoft).

**Sample Preparation for Solid-State NMR.** For membrane samples, 15.2  $\mu\text{mol}$  of **1** (for static  $^{19}\text{F}$  NMR and REDOR measurements) or **2** (for  $^2\text{H}$  NMR) and 35.4  $\mu\text{mol}$  of DMPC (molar ratio 3:7) were dissolved in  $\text{CHCl}_3$ , and the solvent was removed in vacuo for 12 h. The dried membrane film was hydrated with 1 mL of water. After a few minutes of sonication, the suspension was freeze–thawed three times and vortexed to make multilamellar vesicles. The vesicle solution was lyophilized, rehydrated with 30.1  $\mu\text{L}$  of deuterium water (for  $^{19}\text{F}$  NMR and REDOR) or of deuterium-depleted water (for  $^2\text{H}$  NMR), and freeze–thawed three times. The samples were transferred into a 5-mm glass tube (Wilmad) for  $^2\text{H}$  NMR measurement or into 3.2-mm glass tubes (Wilmad) for  $^{19}\text{F}$  NMR and REDOR measurements. All the glass tubes were sealed with epoxy glue. The 3.2-mm glass tube for REDOR measurements was inserted into a 5-mm MAS rotor to measure REDOR.

For measuring the static  $^{19}\text{F}$  NMR of the solid powder of **1**, 15 mg of **1** was packed into a 4-mm MAS rotor, sandwiched by Celite instead of Teflon spacers, and measured without rotation.

**Solid-State NMR Measurements.** All the solid-state NMR spectra were recorded on 300-MHz CMX300 spectrometers (Chemagnetics, Varian, Palo Alto, CA). Static  $^{19}\text{F}$  NMR spectra were acquired at 30  $^\circ\text{C}$  using a 4-mm double-resonance ( $^1\text{H}/^{19}\text{F}$ ) MAS probe without rotation. The DEPTH pulse sequence<sup>14</sup> was applied to reduce  $^{19}\text{F}$  background signals from Teflon capacitor and other  $^{19}\text{F}$  materials used in the probe. The 90 $^\circ$  pulse width was 2.4  $\mu\text{s}$ , the sweep width was 200 kHz, and relaxation delay was 5 s. A total of 51200 transients were accumulated for the membrane sample and 2048 for the solid powder. Continuous wave  $^1\text{H}$  decoupling was applied during acquisition with a decoupling power of 80 kHz. The  $^{19}\text{F}$  chemical shifts were referenced externally to  $\text{CFCl}_3$  (0 ppm).

$^2\text{H}$  spectrum was recorded at 30  $^\circ\text{C}$  with a 5-mm  $^2\text{H}$  static probe using a quadrupolar echo sequence.<sup>32</sup> The 90 $^\circ$  pulse width was 2  $\mu\text{s}$ , interpulse delay was 30  $\mu\text{s}$ , and repetition rate was 0.5 s. The sweep width was 200 kHz, and the number of scans was 80 000.

$^{13}\text{C}\{^{19}\text{F}\}$  REDOR spectra were acquired with a 5-mm triple resonance MAS probe for  $^1\text{H}$ ,  $^{19}\text{F}$ , and  $^{13}\text{C}$ , using xy-4 phase cycling for  $^{19}\text{F}$  irradiations.<sup>33</sup> MAS frequency was 7000 Hz, and rotor temperature was kept at 30  $^\circ\text{C}$ . The  $^1\text{H}$  90 $^\circ$  pulse width was 3.8  $\mu\text{s}$ , and 180 $^\circ$  pulse widths for  $^{13}\text{C}$  and  $^{19}\text{F}$  were 9 and 12  $\mu\text{s}$ , respectively. Contact time for cross-polarization transfer was set to 2.5 ms. The recycle delay was 2.5 s, the sweep width was 30 kHz, and the number of scans was 16 000. The TPPM  $^1\text{H}$  decoupling<sup>34</sup> was applied during acquisition with a decoupling power of 65 kHz. The REDOR dephasing times were 0.571 and 1.143 ms.

(31) Frisch, M. J.; et al. *Gaussian 03*, revision B.05; Gaussian, Inc.: Pittsburgh, PA, 2003.

(32) Davis, J. H.; Jeffrey, K. R.; Bloom, M.; Valic, M. I.; Higgs, T. P. *Chem. Phys. Lett.* **1976**, 42, 390–394.

(33) Gullion, T.; Baker, D. B.; Conradi, M. S. *J. Magn. Reson.* **1990**, 89, 479–484.

(34) Bennett, A. E.; Rienstra, C. M.; Auger, M.; Lakshmi, K. V.; Griffin, R. G. *J. Chem. Phys.* **1995**, 103, 6951–6958.

**Acknowledgment.** We are grateful to Dr. Takashi Iwashita of Suntory Institute for Bioorganic Research and Mr. Mototsugu Doi in our department for advice on solid-state NMR measurements. This work was supported by Grant-In-Aids for Young Scientists (A) (No. 17681027), for Scientific Research (A) (No. 15201048) and (S) (No. 18101010) from MEXT, Japan, and by a grant from the CREST, Japan Science and Technology Corporation.

**Supporting Information Available:** Complete ref 31, tables of Cartesian coordinates and  $^{19}\text{F}$  CSA tensor of the structure shown in Figure 2, REDOR spectra of 6-F-cholesterol in DMPC bilayers, and  $^2\text{H}$  NMR spectra of  $[3\text{-}^2\text{H}]$ cholesterol in powder state and in DMPC. This material is available free of charge via the Internet at <http://pubs.acs.org>.

JA077580L